Reduction of bridge dynamic amplification through adjustment of vehicle suspension damping

N. K. Harris, E. J. OBrien, A. González

Department of Civil Engineering, University College Dublin, Dublin 2, Ireland

Abstract

This paper presents a novel approach to the reduction of short-span bridge dynamic responses to heavy vehicle crossing events. The reductions are achieved through adjustment of the vehicle suspension damping coefficient just before the crossing. Given pre-calculations of the response of a vehicle-bridge system to a set of 'unit' road disturbances, it is shown that a single optimum damping coefficient may be determined for a given velocity and any specified road profile. This approach can facilitate implementation since the optimum damping is selected prior to the bridge and there is no need to continuously vary the damping coefficient during the crossing. The concept is numerically validated using a bridge-vehicle interaction model with several road profiles, both measured and artificially generated. The bridge-friendly damping control strategy is shown to reduce bridge dynamics across a typical range of vehicle velocities, proving most effective for road profiles that induce large vibrations in the vehicle-bridge system.

Keywords: Bridge-friendly, DAF, DAE, dynamic, amplification, damping, suspension.

Corresponding author: Niall Harris
Email: *niall.harris@ucd.ie*
Tel: +353-1-716-7259
Fax: +353-1-716-7399

Nomenclature

$\mathbf{C}$	=	Vehicle damping matrix
$\hat{c}_b$	=	Optimal vehicle damping for bridge crossing
c_{bi}	=	Damping coefficient at axle i
DAE	=	Estimator of DAF
DAF	=	Dynamic Amplification Factor
$d\mathrm{M}(t)$	=	Change in midspan bending moment due to excitation of road profile
$dM_{\mathrm{unit}}(i,t)$	=	Change in midspan bending moment due unit ramp at i^{th} location relative to beam
E	=	Young's modulus of beam
F_{Di}	=	Dynamic tyre force at axle i
$\mathbf{F_D}$	=	Dynamic force vector
F_{Si}	=	Static force at axle i
F_i	=	Total applied force of axle i
G_d	=	Road profile spectral density
h_{unit}	=	Unit ramp height of 0.001m
I	=	Beam cross-section second moment of area
I_S	=	Semi-trailer pitch moment of inertia
I_T	=	Tractor pitch moment of inertia
j	=	Mode number
$\mathbf{K}$	=	Vehicle stiffness matrix
k_i	=	Suspension spring stiffness at axle i
k_{ti}	=	Tyre stiffness at axle i
L	=	Bridge span
$\mathbf{M}$	=	Vehicle mass matrix

$M(x,t)$ = Bending moment

$M_b(x,t)$ = Bending moment due to vibration of bridge

$M_f(t)$ = Midspan bending moment due to passage of vehicle over smooth profile

$M_v(x,t)$ = Bending moment due to instantaneous axle forces

M_0 = Maximum static midspan bending moment

m_S = Semi-trailer body mass

m_T = Tractor body mass

m_i = Mass of axle i

N = Number of intervals/ramps

n = Wavenumber

$q_{(j)}(t)$ = Normalised deflection for mode j and time t

$r_i(t)$ = Road elevation under axle i at time t

s_i = Ramp scale factor for two adjacent measurement points

t = Time

w = Constant relating to pavement roughness

x = Distance along bridge (relative to $x = 0$ at the start of the bridge)

x_i = Distance of axle i along bridge

$\mathbf{y}$ = Displacement vector of vehicle model

y_S = Semi-trailer displacement

y_T = Tractor displacement

$y_b(x,t)$ = Bridge displacement

y_i = Displacement of axle i

Δt = Time step

ε_i = Parameter indicating whether axle i is on or off the bridge

ζ_d = Bridge damping parameter

θ_S = Semi-trailer pitch

θ_T = Tractor pitch

μ = Mass per unit length

$\omega_{(1)}$ = Beam 1st natural frequency

1. Introduction

Freight transport has grown by over 18% in the European Union in the 7 year period from 1995 to 2002 [1], a growth trend which seems likely to continue in the medium term. In order to satisfy the increasing demand for freight transport capacity on roads, it will be necessary to have more vehicles and/or heavier vehicles. Heavier vehicles could involve more axles of the same weight (e.g., current 5@8 tonnes to future 6@8 tonnes) thereby having a modest effect on the rate of pavement deterioration. However, any increase in Gross Vehicle Weight (GVW) would tend to increase the characteristic traffic loading on bridges. The vibrations induced by heavy moving loads can increase the maximum internal stresses in bridges, affecting their safety and serviceability [2] and while it is relatively inexpensive to provide additional load carrying capacity during the design stage of a highway bridge, the cost of upgrading or strengthening existing bridges is significant.

In this paper, bridge response is defined in terms of the Dynamic Amplification Factor (DAF), which is a measure of the maximum total response resulting from the interaction of moving loads and the bridge structure, as a proportion of the maximum static response [3]. It is known that the DAF due to a given vehicle load is strongly dependent on a number of system properties such as bridge and vehicle parameters, vehicle velocity and approach pavement roughness [4, 5, 6, 7].

Kirkegaard et al. [8] performed a review of the DAF values used in various national codes. It was noted that for assessment of bridges, the dynamic allowance, where specified, varies significantly from code to code. The US AASHTO specification is governed by pavement condition, allowing for mean values of up to 1.30 with

standard deviations of up to 0.3. It was also noted that the Canadian allowance is calculated according to GVW, with a mean value of 1.106 (standard deviation 0.104) specified for 40t vehicles. In the UK, a dynamic allowance is made for up to 80% of the heaviest axle of a vehicle [9]. For short spans with poor pavement condition, Cooper [10] recommends a mean dynamic allowance of up to 1.13 with a standard deviation of 0.15. This suggests that truck weights can be significantly increased (or bridge upgrading/replacement costs reduced) if the allowance for dynamics in such bridges can be minimised. Certain road networks, such as the Danish Blue Road Network [11], are pre-classified for heavy vehicles, with load-carrying capacity of bridges in the network calculated and available. In this context, the use of smart, bridge-friendly vehicle suspensions could allow heavy vehicles to traverse bridges that were previously deemed below classification, or for increased payloads to be permitted across sections of the bridge network.

This paper presents a novel approach to effecting a reduction in the dynamic loading of bridges, particularly short spans, through the use of real-time control of vehicle damping within an Intelligent Vehicle Bridge System (IVBS). Assuming that a communication link is available between the vehicle and the bridge, the control strategy selects the optimum suspension damping coefficient for the vehicle crossing event.

2. Active/Semi-active suspension strategies

In recent years, there has been considerable research effort on the development of methods for mitigating the vibration of bridges under a moving load or set of moving loads. Patten *et al* [12] fitted a semi-active actuator to an existing bridge, reducing

magnitudes of dynamic loading, greatly extending the predicted service life. The use of tuned mass dampers has been shown by Kwon *et al* [13] to be an effective means of passive vibration control. However, such methods require considerable installation or retrofitting effort on the bridge deck giving rise to the alternative solution of equipping the vehicle with a means of bridge friendly control. Further, such an approach is more consistent with a policy of allowing vehicles with the equipment installed to carry heavier loads.

The use of advanced suspension systems incorporating controllable dampers or actuators has been considered by numerous authors. Such systems can be used both to reduce sprung mass accelerations, a criterion of driver comfort, and as an approach to mitigating dynamic tyre forces applied to a pavement or bridge deck [2, 14, 15]. Recently, the specific concept of bridge friendly suspensions has been investigated. Chen et al. [16] conducted a study to determine the effects of two semi-active suspension control strategies on the dynamic response of a bridge, concluding that mitigation of bridge response through tuning of suspension parameters is feasible. Giraldo and Dyke [17] considered the active and semi-active control of the damper on a moving oscillator traversing an elastic beam, based on dynamic measurements of acceleration and displacement at specified points on the beam. The concept of an IVBS has been proposed by DeBrunner *et al* [18] as a means of both reducing bridge response and providing system status information for vehicle crossings. An integrated system is described in which the traversing vehicle applies an active damping force through an actuator in order to reduce bridge vibrations. The active control strategy proposed was dependent on the relaying of continuous measurements of bridge vibration to the suspension controller.

The suspension control strategy presented herein seeks to minimise bridge DAF within the context of an IVBS. Dynamic response of the bridge is mitigated, based on a prior forecast of the vehicle-bridge interaction. A significant advantage of the control strategy is that the damping coefficient is set prior to the arrival of the vehicle and remains constant throughout the crossing event; eliminating the need to continuously vary vehicle damping over what is usually a short time. For this purpose, two assumptions are made:

- The bridge response due the vehicle running over a set of unit ramps spaced along the bridge is known and is stored for a range of velocities in a database available to the suspension controller;
- The road profile, both on the bridge deck and the immediate approach is relayed to the vehicle prior to the crossing event.

This novel control strategy uses an extension of the concept of Dynamic Amplification Estimate (DAE), which allows an approximate calculation of DAF [19], to calculate optimal vehicle suspension damping values without the need to solve complex differential equations.

3. Vehicle Bridge Interaction

This section describes the numerical implementation of the vehicle-bridge-pavement interaction model used to determine optimal damping for the crossing. The interaction process is implemented with MatLab Simulink software [20]. Initially surface profile heights, $r_i(t)$, are input to each axle of the vehicle and the vehicle tyre forces, $F_i(t)$, are

computed. The bridge model is subjected to each axle load as the vehicle traverses the beam and the midspan bending moment is used to calculate DAF for the crossing event. For each incremental time step, Δt, the bridge deflection under each axle, $y_b(x,t)$, is returned to the vehicle model to calculate dynamic tyre force.

3.1 Vehicle Model

The vehicle model used for simulation of dynamic tyre forces imparted to the bridge is a 5-axle multiple degree of freedom articulated truck, illustrated in Fig. 1. This is a typical European truck configuration which is known to contribute to critical loading cases for short and medium span bridges [21]. The effect of vehicle roll on bridge dynamics is not considered; analysis is in the pitch plane only. Both the tractor and semi-trailer are assumed to be rigid bodies connected at a hitching point, *W*, the so-called 'fifth wheel'. The two bodies are supported by five sets of suspensions, two located on the tractor (front and rear) and a tridem suspension on the semi-trailer. The equations of motion are based on the formulation provided by ElMadany [22] for the ride behaviour of an articulated 3-axle tractor/semi-trailer.

Accounting for the constraints imposed by the hitching point on the motion of the rigid bodies, the vehicle model has eight independent degrees of freedom: bouncing (y_T) and pitching (θ_T) motion of the tractor centre of gravity, pitching motion (θ_S) of the semi-trailer centre of gravity and vertical hop (y_1, y_2, y_3, y_4, y_5) motions of each axle assembly. The drive axle at the rear of the tractor is chosen as the axle with the capability of providing a prescribed damping coefficient, $\hat{c}_b$, and hence a prescribed damping force, F_d, to the system. The equations of motion for the vehicle model can be expressed in matrix form as:

$$\mathbf{M}\ddot{\mathbf{y}} + \mathbf{C}\dot{\mathbf{y}} + \mathbf{K}\mathbf{y} = \mathbf{F_D} \tag{1}$$

where $\{y\}$, $\{\dot{y}\}$ and $\{\ddot{y}\}$ are the vectors of displacements, velocities and accelerations respectively and

$$\mathbf{y}^T = \{y_T \quad q_T \quad q_S \quad y_1 \quad y_2 \quad y_3 \quad y_4 \quad y_5\} \tag{2}$$

And, $\{F_D\}$, the force vector yields the dynamic force component given by:

$$\mathbf{F_D}^T = \{0 \quad 0 \quad 0 \quad -F_{D1} \quad -F_{D2} \quad -F_{D3} \quad -F_{D4} \quad -F_{D5}\} \tag{3}$$

The first three terms of the force vector correspond to the pitching and heaving degrees of freedom of the tractor and semi-trailer and the other terms are:

$$F_{Di}(t) = k_{ti}(y_i(t) - y_b(x_i,t) - r_i(t)) \qquad i = 1,2,3,4,5 \tag{4}$$

where $y_i(t)$ is the i^{th} axle displacement (Fig. 1) and $y_b(x_i,t)$ and $r_i(t)$ are the displacements of the beam and road profile respectively underneath the axle. The mass, damping and stiffness matrices are given in Appendix A, along with the constraint equations for the vehicle motion. Combining the dynamic tyre force for each axle with the corresponding static weight, F_{Si}, yields the total axle force applied to the bridge deck, F_i:

$$F_i(t) = F_{Si} + F_{Di} \qquad i = 1,2,3,4,5 \tag{5}$$

Table 1 provides a full list of the model parameter values used. Suspension parameters are chosen to represent the behaviour of air-sprung suspensions with parallel viscous dampers [23]. It is also assumed that the three axles of the tridem share the rear static load equally, as load sharing mechanisms are common with multi-axle heavy vehicle suspensions [2]. Since the vertical deflections and pitching motions are assumed to be small relative to the overall vehicle geometry, the springs in the suspension systems as well as the vehicle tyres are modelled with linear characteristics.

It is clear from the assumptions made that the modelling approach neglects certain aspects of heavy vehicle ride behaviour. The use of a pitch plane model, which neglects rolling effects, is considered sufficient as it has been noted that under typical highway operating conditions, the effect of roll on dynamic tyre forces is minimal [2]. Furthermore, it is noted that whilst the non-linearities associated with suspension component behaviour, such as Coulomb friction between linkages and the adiabatic compression of fluid in the air spring, are not considered, a linearised ride model still provides a useful tool for assessing the performance potential of a vehicle suspension [22]. As such, the model is considered sufficient for the demonstration of the concept of the bridge-friendly suspension presented herein.

3.2 Bridge Model

A simply supported beam subjected to five time varying forces (F_i), corresponding to the vehicle axle loads, is used to obtain bridge response to the vehicle crossing event.

The solution for the displacement of a beam of length L [24] at location x and time t, may be expressed as an expansion in terms of the generalised coordinates, $q_{(j)}(t)$.

$$y_b(x,t) = \sum_{j=1}^{\infty} q_{(j)}(t) \sin \frac{j\pi x}{L} \tag{6}$$

These generalised coordinates are determined by the solution to:

$$\ddot{q}_{(j)}(t) + 2\zeta_d \omega_{(1)} \dot{q}_{(j)}(t) + \omega_{(1)}^2 q_{(j)}(t) = \frac{2}{mL} \sum_{i=1}^{5} e_i F_i(t) \sin \frac{j\pi x_i}{L} \tag{7}$$

where $F_{ti}(t)$ is the i^{th} axle force imparted to the bridge deck within the domain specified by function ε_i:

$$e_i = \begin{cases} 1 & \text{for} \quad 0 \le x_i \le L \\ 0 & \text{for} \quad x_i \le 0; x_i \ge L \end{cases} \tag{8}$$

and the first natural frequency of the beam is given by:

$$\omega_{(1)} = \left(\frac{\pi}{L}\right)^2 \sqrt{\frac{EI}{m}} \tag{9}$$

The bending moment response of the beam, $M(x,t)$, at a bridge location x and instant t since the vehicle entered the bridge, can be expressed as the sum of two components; the response due to the instantaneous vehicle forces applied to the beam, $M_v(x,t)$, and the response due to the inertial forces of the beam, $M_b(x,t)$:

$$M(x,t) = M_v(x,t) + M_b(x,t) \tag{10}$$

$$M_v(x,t) = \sum_{i=1}^{5} M_{vi} \quad \text{where} \quad \begin{cases} M_{vi} = e_i F_i (L - x_i)\dfrac{x}{L} & \text{for } x_i \geq x \\ M_{vi} = e_i F_i (L - x)\dfrac{x_i}{L} & \text{for } x_i \leq x \end{cases} \tag{11}$$

$$M_b(x,t) = -\sum_{j=1}^{\infty} \frac{mL^2}{p^2}\frac{1}{j^2}\ddot{q}_{(j)}(t)\sin\frac{jp x}{L} \tag{12}$$

The DAF is then determined by taking the maximum value of the midspan bending moment ($x=L/2$), divided by M_0, the maximum static load effect induced at bridge midspan by the vehicle.

$$DAF = \frac{1}{M_0}\max_t [M(L/2,t)] \quad \forall t \tag{13}$$

A significant advantage of using Equation (10) to determine the bridge dynamic response is that the solution has been shown to converge rapidly for a relatively low number of modes of vibration [24], to the extent that the first mode contribution differs from the contribution of five modes or greater by less than 3%. This is particularly applicable for vehicle velocities lower than the critical one of the beam. For the purposes of this study, the first six modes of vibration of the beam are considered.

It will be shown in section 4 that bridge dynamic response may be mitigated through selection of an optimal vehicle damping coefficient. As such, it is anticipated that the effect of the method would be maximised for short-span bridges in which the ratio of GVW to overall bridge mass is greater, increasing the potential of generated tyre forces to influence bridge dynamic response. For this purpose, bridge parameters are selected to represent a 10 m span slab bridge of constant cross-section, with a first natural frequency of 10 Hz, mass per unit length of 17125 kg/m, and 1.5% damping.

3.3 Road Profile Generation and Filtering

In addition to measured profiles, two artificially generated profiles are used for this study. The spectral densities of these profiles, $G_d(n)$, are generated using British Standard classifications [25] for road roughness, given by:

$$G_d(n) = G_d(n_0)\left(\frac{n}{n_0}\right)^{-w} \tag{14}$$

where n is the wavenumber in cycles/m, n_0 = 0.1 cycles/m and $G_d(n_0)$ and w are constants related to the surface roughness of the pavement. The spectral density is inverse Fourier transformed to produce a discrete set of points representing the profile height, $r(t)$, at regular finite intervals. Two profiles are generated, the first having a roughness coefficient of $G_d(n_0) = 32 \times 10^{-6}$ m^3/cycle, corresponding to a class 'B' road (good quality highway). The second profile is a class 'C' pavement (standard road) with a roughness coefficient of $G_d(n_0) = 64 \times 10^{-6}$ m^3/cycle. The lengths of randomly generated road profile are then passed through a moving average filter [26] to

simulate the envelopment of short wavelength disturbances by the tyre contact patch. A base wavelength of 0.3 m was chosen for this purpose.

4. Principle of Operation

This section explains the DAE and extends the concept for use in reduction of bridge DAF.

For an irregular (non-smooth) surface and small bridge deflections, the bridge bending moment at midspan, $M(L/2, t)$, given by Equation (10), may be approximated by:

$$M(t) \; ; \quad M_f(t) + dM(t) \tag{15}$$

where $M_f(t)$ is the bridge response due to the passage of the vehicle over a smooth profile and $dM(t)$ is the change in overall response due to the excitation of the vehicle by the irregular profile. The contribution of the road surface irregularity is illustrated by Fig. 2, which shows the response of the bridge described in section 3.2 to the passage of the heavy vehicle model at 72km/hr, excited by an irregular road profile, generated according to section 3.3.

Li et al [19] have shown that this value $dM(t)$ may be calculated by summing the changes in response of the vehicle-bridge interaction system to N equally spaced ramps, 0.1 m apart, that together may be used to represent the irregular profile. The contribution of each ramp is determined by scaling the predetermined response of the

vehicle bridge system to a unit ramp, where a unit ramp is defined as a fall of 0.001 m in 0.1 m, at that location. Hence, $dM(t)$ becomes:

$$dM(t) \approx \sum_{i=1}^{N} s_i dM_{\text{unit}}(i,t) \tag{16}$$

where s_i is the ramp scale factor or difference in road heights between location i *and* $i+1$, divided by the unit height, $h_{\text{unit}} = 0.001$ m:

$$dM(t) \approx \sum_{i=1}^{N} s_i dM_{\text{unit}}(i,t) \tag{17}$$

The suspension control strategy seeks to determine the optimum damping coefficient setting in order to minimise bridge DAF. Hence, the overall response determined using equations (15) and (16) is extended to account for variable damping coefficients:

$$M(c_b,t) = M_f(c_b,t) + \sum_{i=1}^{N} s_i dM_{\text{unit}}(i,c_b,t) \tag{18}$$

Taking the maximum response over the time of crossing of the vehicle, $\max_t M(t)$, and dividing it by the maximum static response, M_o, yields the DAE for a particular velocity and damping rate, c_b. The DAE now provides a means of both predicting DAF, defined by Equation (13) and of selecting the optimum vehicle damping coefficient, $\hat{c}_b$, within practical minimum and maximum values, to minimise dynamic amplification. The need to conduct a full interaction simulation is eliminated

and replaced by Equations (17) and (18), which are simple summations of predetermined responses of the bridge.

4.1 Example of Concept

The following example shows how the control strategy applies the DAE concept (based on a prior knowledge of the road profile, vehicle and bridge dynamic properties) to adjust the vehicle damping, c_b, so as to achieve minimum bridge DAF. Consider the simplified road profile shown in Fig. 3, consisting of three ramps with different gradients at arbitrary locations relative to the start of the beam. It is possible to discretise any measured or artificially generated road profile in this manner. It should be noted that *Ramp1*, while not located on the bridge itself, can excite the vehicle model prior to crossing, altering the initial conditions and hence, the bridge response. Hence, it is necessary to consider the roughness in the approach as well as on the bridge to accurately predict the response to the vehicle.

The change in bending moment, dM (Equation (15)), due to each individual ramp is found by scaling the response to a unit ramp, dM_{unit} (Equation (16)). These three responses are added together and combined with the bending of the bridge due to the passage of the vehicle over a perfectly smooth profile, M_f (Equation (15)). The concept is illustrated by Fig. 4, which shows the contribution of each individual ramp to the bridge response, $dM(t)/M_o$, for a vehicle crossing at 86 km/hr. It is clear that certain ramps induce greater changes due to a combination of location and gradient, the most significant ramp in this case being *Ramp3*. Fig. 5 compares the overall bending moment due to a smooth profile ($M_f(t)$), to the 3 ramps ($dM(t)$) and to the combined contributions of the three discretized ramps. The DAE is increased from

1.10 to 1.25 due to the effects of the uneven surface, an increase of 150% in the dynamic increment (i.e. the dynamic response in excess of the corresponding static value of 1.0).

By extending this analysis to include the change in DAE due to damping coefficient in the 2nd axle as well as unit ramp location, as described in Equation (18), it is possible to calculate the optimum damping, $\hat{c}_b$, for a vehicle crossing event. Fig. 6 shows a plot of DAE and DAF versus damping coefficient, c_b, for the test profile shown in Fig. 3 at a vehicle velocity of 72 km/hr. It can be seen that the estimator method (DAE) provides an excellent prediction of the trend obtained by full simulation (DAF), yielding an optimum damping coefficient (within a minimum and maximum of 5 kNs/m and 45 kNs/m respectively) of 13.0 kNs/m (compared to 12.8 kNs/m from full simulation with DAF obtained using Equations (10) and (13)).

5. Validation

For six individual road profiles, the method introduced in section 4 is tested. Bridge response to the vehicle crossing event for all ramp locations and damping coefficients is determined for the same 10 m simply supported beam test model. The road profiles relative to the start of the bridge (0 m), illustrated in Fig. 7, consist of two measured profiles from the Netherlands (NL1, NL2), two further measured profiles from Slovenia (section of main road Trbovlje Hrastnik, at a bridge over the Sava river), (SI1, SI2) and two artificially generated profiles, as described in section 3.3 (AR1, AR2).

The bridge-friendly control strategy is tested across a range of truck velocities from 60 – 120 km/hr and compared with the response for a fixed (passive) damping coefficient of 10 kNs/m. The controllable suspension is studied for a range of damping coefficients between maximum and minimum allowable values of 5 kNs/m and 45 kNs/m respectively. Fig. 8(a) shows the optimum damping coefficient selected by the control strategy for profile NL1 (Fig. 7(a)) while the corresponding reduction in DAF from the passive value is shown in Fig. 8(b). This road profile is relatively smooth and as such, does not excite the vehicle suspension. Consequently the effect of pavement roughness on bridge DAF is relatively low, with other critical factors such as vehicle velocity, axle spacing and static load distribution taking on greater significance. The low suspension excitation induced by the profile also affects the magnitudes of damping force that the suspension generates, hence undermining the ability of the vehicle suspension to effectively oppose the bridge vibration. As a result, the maximum bridge DAF which occurs across the velocity range is only marginally reduced from 1.10 to 1.09.

The effect of the bridge-friendly control strategy on profile SI1 (Fig. 7(c)) is illustrated in Figs. 9(a) and 9(b), again showing the predicted optimum damping coefficient and reductions in DAF respectively. In contrast to profile NL1, the profile is relatively uneven, inducing greater levels of vehicle vibration and consequently, greater bridge vibration. As such, it can be seen that optimising the damping coefficient in the 2nd axle has an increased effect in changing the system response, reducing overall DAF across the velocity range from 1.74 to 1.54. This equates to an overall reduction of 12% in DAF, or a 27% reduction in the dynamic increment due to the moving loads.

In general, magnitudes of DAF are reduced by the control strategy through an alteration of the oscillating bridge dynamic component of overall bending moment, M_b, given by Equation (12). If the magnitude of this component is large, then large values of DAF will occur if there is constructive interference between this component and the vehicle force component, M_v, given by Equation (11), at the time at which DAF occurs. However, cases in which there is destructive interference between M_b and M_v at the instant at which DAF occurs, will yield low values of DAF for large magnitudes of M_b. In this context, the variation of vehicle damping reduces DAF in three ways. When the DAF is due to constructive interference, a high damping coefficient is specified, which has the effect of reducing the magnitude of the oscillating bridge dynamic component, M_b, through increased damping forces from the vehicle suspension, hence reducing overall DAF. Second, in cases where destructive interference between M_v and M_b is present at the instant of DAF, a low damping coefficient is specified. Reduced vehicle damping forces induce greater magnitudes of M_b, encouraging greater destructive interference between the two components of bending moment, hence reducing DAF. Finally, an intermediate coefficient can be specified, such as at 65 km/hr in Fig. 9(a), as an optimum solution to the combination of both effects. Increased damping from the minimum value limits the amplitude of M_b, but in some cases, as damping increases, a phase shift also occurs in the same component, subsequently resulting in constructive interference between M_v and M_b at the time of DAF, hence increasing its magnitude. Under these circumstances, the intermediate value is chosen as the optimum compromise between both effects.

A summary of the effects of the bridge-friendly control strategy on the remainder of the road profiles considered is given in Table 2. Reductions in DAF are achievable for all profiles, though the effect tends to be greater on those rougher profiles which cause high values of DAF. This is consistent with the fact that for rougher roads, the vehicle suspension is subjected to greater excitation by the road profile, thus generating higher damping forces, capable of altering the dynamic bridge response. It is noted that for one of the smoother profiles (NL2), while DAF is reduced by less than 0.02, this equates to an elimination of 16% of the dynamic increment due to the passage of the vehicle.

While reductions in bridge response are desirable, any adverse effects of the bridge-friendly control strategy on vehicle ride performance should be considered. Commonly used criteria for the characterisation of suspension performance in terms of road damage [2, 27] and driver comfort [2, 14, 27] are measurements of root mean square (RMS) tyre force and RMS body acceleration respectively. For certain profiles (SI1, AR2), the maximum RMS body acceleration experienced is marginally increased by up to 2.0%, though levels remained within accepted limits [28]. The RMS tyre force imparted by the rear tractor axle, with the controllable damper, remains largely unaffected.

6. Conclusions

A new approach to the reduction of bridge dynamic excitation through control of the vehicle suspension is presented. This bridge-friendly control strategy is validated using a multi-axle articulated vehicle model traversing a simply supported Euler Bernoulli beam. It is shown that it is possible to quickly estimate the dynamic

response of the bridge to a vehicle excited by any given road profile, provided a prior knowledge exists of the response of the vehicle-bridge system to a set of 'unit ramp' disturbances at regular intervals on and near the bridge. The method is extended to account for variable suspension damping, allowing for the selection of a single, optimum damping coefficient for a crossing event.

The effect of the bridge-friendly control strategy is investigated for several measured and artificially generated road profiles. In all cases, maximum bridge DAF is reduced across a typical range of vehicle velocities due to the new approach. The effect is generally more pronounced for rougher profiles with reductions of up to 40% of the dynamic increment achieved. For relatively smooth profiles, the contribution of road roughness to overall DAF is lessened, and the achievable reductions tend to be smaller. It is also noted that RMS tyre forces and RMS body accelerations are largely unaffected by the bridge-friendly suspension.

Acknowledgements

The authors wish to acknowledge the continued financial support provided by the Irish Research Council for Science, Engineering and Technology (IRCSET) *Embark Initiative*.

Appendix A: Mass, Stiffness and Damping Matrices for Vehicle Model

The following section details the mass, stiffness and damping matrices, used in Equation (1) to describe the vehicle ride behaviour. As previously stated, the formulation is based on the 6 degree-of-freedom vehicle model used by El-Madany [22] and utilises the same compatibility conditions as follows:

$$y_S = y_T + b_7 q_T + b_6 q_S \tag{A1}$$

$$x_S = x_T + a_1 q_T + a_2 q_S \tag{A2}$$

$$x_T = \frac{m_7}{m_6 + m_7}(a_1 q_T - a_2 q_S) \tag{A3}$$

where

$$\begin{aligned} m_6 &= m_S + m_3 + m_4 + m_5 \\ m_6 &= m_T + m_1 + m_2 \end{aligned} \tag{A4}$$

Given these constraints, the mass matrix, **M**, may then be expressed as:

$$\mathbf{M} = \begin{bmatrix} (m_T + m_S) & b_7 m_s & b_6 m_s & 0 & 0 & 0 & 0 & 0 \\ b_7 m_s & \left(I_T + b_7^2 m_s + \frac{m_6 m_7}{m_6 + m_7} a_1^2\right) & \left(b_6 b_7 m_s - \frac{m_6 m_7}{m_6 + m_7} a_1 a_2\right) & 0 & 0 & 0 & 0 & 0 \\ b_6 m_s & \left(b_6 b_7 m_s - \frac{m_6 m_7}{m_6 + m_7} a_1 a_2\right) & \left(I_S + b_6^2 m_s + \frac{m_6 m_7}{m_6 + m_7} a_2^2\right) & 0 & 0 & 0 & 0 & 0 \\ 0 & 0 & 0 & m_1 & 0 & 0 & 0 & 0 \\ 0 & 0 & 0 & 0 & m_2 & 0 & 0 & 0 \\ 0 & 0 & 0 & 0 & 0 & m_3 & 0 & 0 \\ 0 & 0 & 0 & 0 & 0 & 0 & m_4 & 0 \\ 0 & 0 & 0 & 0 & 0 & 0 & 0 & m_5 \end{bmatrix} \tag{A5}$$

And the damping, **C**, and stiffness, **K**, matrices are:

$$\mathbf{C} = \begin{bmatrix} c_{b1}+c_{b2}+c_{b3}+c_{b4}+c_{b5} & -b_1c_{b1}+b_2c_{b2}+b_7(c_{b3}+c_{b4}+c_{b5}) & (b_6+b_3)c_{b3}+(b_6+b_4)c_{b4}+(b_6+b_5)c_{b5} & -c_{b1} & -c_{b2} & -c_{b3} & -c_{b4} & -c_{b5} \\ -b_1c_{b1}+b_2c_{b2}+b_7(c_{b3}+c_{b4}+c_{b5}) & b_1^2c_{b1}+b_2^2c_{b2}+b_7^2(c_{b3}+c_{b4}+c_{b5}) & b_7\left((b_6+b_3)c_{b3}+(b_6+b_4)c_{b4}+(b_6+b_5)c_{b5}\right) & b_1c_{b1} & -b_2c_{b2} & -b_7c_{b3} & -b_7c_{b4} & -b_7c_{b5} \\ (b_6+b_3)c_{b3}+(b_6+b_4)c_{b4}+(b_6+b_5)c_{b5} & b_7\left((b_6+b_3)c_{b3}+(b_6+b_4)c_{b4}+(b_6+b_5)c_{b5}\right) & (b_6+b_3)^2c_{b3}+(b_6+b_4)^2c_{b4}+(b_6+b_5)^2c_{b5} & 0 & 0 & -(b_6+b_3)c_{b3} & -(b_6+b_4)c_{b4} & -(b_6+b_5)c_{b5} \\ -c_{b1} & b_1c_{b1} & 0 & c_{b1} & 0 & 0 & 0 & 0 \\ -c_{b2} & -b_2c_{b2} & 0 & 0 & c_{b2} & 0 & 0 & 0 \\ -c_{b3} & -b_7c_{b3} & -(b_6+b_3)c_{b3} & 0 & 0 & c_{b3} & 0 & 0 \\ -c_{b4} & -b_7c_{b4} & -(b_6+b_4)c_{b4} & 0 & 0 & 0 & c_{b4} & 0 \\ -c_{b5} & -b_7c_{b5} & -(b_6+b_5)c_{b5} & 0 & 0 & 0 & 0 & c_{b5} \end{bmatrix}$$

(A6)

$$\mathbf{K} = \begin{bmatrix} k_1+k_2+k_3+k_4+k_5 & -b_1k_1+b_2k_2+b_7(k_3+k_4+k_5) & (b_6+b_3)k_3+(b_6+b_4)k_4+(b_6+b_5)k_5 & -k_1 & -k_2 & -k_3 & -k_4 & -k_5 \\ -b_1k_1+b_2k_2+b_7(k_3+k_4+k_5) & b_1^2k_1+b_2^2k_2+b_7^2(k_3+k_4+k_5) & b_7\left((b_6+b_3)k_3+(b_6+b_4)k_4+(b_6+b_5)k_5\right) & b_1k_1 & -b_2k_2 & -b_7k_3 & -b_7k_4 & -b_7k_5 \\ (b_6+b_3)k_3+(b_6+b_4)k_4+(b_6+b_5)k_5 & b_7\left((b_6+b_3)k_3+(b_6+b_4)k_4+(b_6+b_5)k_5\right) & (b_6+b_3)^2k_3+(b_6+b_4)^2k_4+(b_6+b_5)^2k_5 & 0 & 0 & -(b_6+b_3)k_3 & -(b_6+b_4)k_4 & -(b_6+b_5)k_5 \\ -k_1 & b_1k_1 & 0 & k_1 & 0 & 0 & 0 & 0 \\ -k_2 & -b_2k_2 & 0 & 0 & k_2 & 0 & 0 & 0 \\ -k_3 & -b_7k_3 & -(b_6+b_3)k_3 & 0 & 0 & k_3 & 0 & 0 \\ -k_4 & -b_7k_4 & -(b_6+b_4)k_4 & 0 & 0 & 0 & k_4 & 0 \\ -k_5 & -b_7k_5 & -(b_6+b_5)k_5 & 0 & 0 & 0 & 0 & k_5 \end{bmatrix}$$

(A7)

References

[1] European Union Energy and Transport in Figures 2004, European Commission, 2004, http://europa.eu.int/comm/dgs/energy_transport/figures/pocketbook/.

[2] D. Cebon, Handbook of Vehicle-Road Interaction, Swets & Zeitlinger, 1999.

[3] S.P. Brady, The Influence of Vehicle Velocity on Dynamic Amplification in Highway Bridges, PhD Thesis, University College Dublin, 2004.

[4] DIVINE Programme, OECD, Dynamic Interaction of Heavy Vehicles with Roads and Bridges, DIVINE Concluding Conference, Ottawa, Canada, 1997.

[5] M.F. Green, D. Cebon, Dynamic interaction between heavy vehicle and highway bridges, *Computers and Structures* 62 (1997) 253–264

[6] G. T. Michaltsos and T. G. Konstantakopoulos, Dynamic Response of a Bridge With Surface Deck Irregularities, *Journal of Vibration and Control*, 6 (2000) 667-689.

[7] A.V. Pesterev, L.A. Bergman, C.A. Tan, A novel approach to the calculation of pothole-induced contact forces in MDOF vehicle models, *Journal of Sound and Vibration*, 275 (2004) 127-149

[8] P.H. Kirkegaard, S.R.K. Nielsen, I. Enevoldsen, Heavy vehicles on minor highway bridges – A literature review, Structural Reliability Theory Paper No. 169, Department of Building Technology and Structural Engineering, Aalborg University, Denmark, 1997.

[9] BD 21/97, The Assessment of Highway Bridges and Structures. Design Manual for Roads and Bridges, Vol. 3, Section 4, Part 3. HMSO, London, 1997.

[10] D.I. Cooper, Development of short span bridge-specific assessment live loading, in: P.C. Das (Ed.), *Safety of Bridges*, Thomas Telford, London, 1997.

[11] I. Enevoldsen, M. Sloth, J. Lauridsen, Danish guideline for probability based assessment of bridges, *Proc. IABMAS '04,* Kyoto, Japan, pp. 599 - , 2004.

[12] W.N. Patten, J. Sun, G. Li, J. Kuehn, G. Song, Field test of an intelligent stiffener for bridges at the I-35 Walnut Creek bridge, *Earthquake Engineering and Structural Dynamics*, 28 (1999) 109-126.

[13] H.C. Kwon, M.C., Kim, I.W. Lee, Vibration control of bridge under moving loads, *Computers and Structures*, 66 (1998) 473-480.

[14] M. Valášek, M. Novák, Z. Šika, O. Vaculĭn, Extended Ground-Hook – New Concept of Semi-Active Control of Truck's Suspension, *Vehicle System Dynamics*, 27 (1997) 289-303.

[15] M. Valášek, W. Kortum, Z. Šika, L. Magdolen, O. Vaculĭn, Development of Semi-Active Road-Friendly Truck Suspensions, *Control Engineering Practice*, 6 (1998) 735-744.

[16] Y. Chen, C.A. Tan, L.A. Bergman, T.C. Tsao, Smart suspension systems for bridge-friendly vehicles, *Proceedings of SPIE* - Volume 4696, Smart Structures and Materials 2002: Smart Systems for Bridges, Structures, and Highways, S.-C. Liu, Darryll J. Pines, Editors, pp. 52-61, June 2002

[17] D. Giraldo, S.J. Dyke, Control of a moving oscillator on an elastic continuum using smart dampers, *Proc. American Control Conference,* Anchorage, AK, pp. 3058 – 3063, 2002.

[18] V. DeBrunner, D. Zhou, M. Ta, Adaptive vibration control of a bridge and heavy truck, *Intelligent Vehicles Symposium, 2003, Proceedings*, IEEE, 2003

[19] Y. Li, E.J. O'Brien, A. González, The Development of a Dynamic Amplification Estimator for Bridges with Good Road Profiles, submitted to the *Journal of Sound and Vibration*, 2005.

[20] Using Simulink, The Mathworks, Inc., USA, 2003.

[21] S. Grave, Modelling of Site-Specific Traffic Loading on Short to Medium Span Bridges, PhD Thesis, Trinity College Dublin, 2001.

[22] M. M. El-Madany, Design optimization of truck suspensions using covariance analysis, *Computers and Structures*, 28 (1988), No. 2, pp. 241-246.

[23] P. S. Fancher, R. D. Ervin, C. B.Winkler, T. D. Gillespie, A factbook of the mechanical properties of the components for single-unit and articulated heavy trucks, Technical Report UMTRI-86-12, University of Michigan Transportation Research Institute, Ann Arbor, MI, USA, 1986.

[24] L. Fryba, Vibration of Solids and Structures under Moving Loads, Noordhoff, Groningen, Netherlands, 1972.

[25] British Standards Institution, BS7853:1996 Mechanical Vibration – Road Surface Profiles – Reporting of Measured Data, Milton Keynes, BSI, 1996.

[26] M.W. Sayers, S.M. Karamihas, Interpretation of Road Roughness Profile Data – Final Report, University of Michigan Transportation Research Institute (UMTRI) Report 96-19, 1996.

[27] K. Yi, J.K. Hedrick, Active and semi-active heavy truck suspension to reduce pavement damage, *SAE Trans,* 892486 (SP-802), pp.29-36, 1989.

[28] ISO 2631-1, Mechanical vibration and shock – Evaluation of human exposure to whole-body vibration – Part 1: General requirements, 1997

Fig. 1. Tractor semi-trailer vehicle model

Fig. 2. Normalised midspan bending moment due to vehicle crossing event (--- Smooth profile ── Irregular profile)

Fig. 3. Simple road profile consisting of a series of scaled unit ramps

Fig. 4. Change in bending moment due to contribution of each individual ramp (····· ramp 1 ---- ramp 2 ── ramp 3)

Fig. 5. Application of DAE concept: Bending moment (····· due to road unevenness (all 3 ramps) ---- due to smooth profile ── combined response)

Fig. 6. Determination of optimum damping coefficient (── full simulation (DAF) +++ estimator method (DAE))

Fig. 7. Road profiles (a) NL1 (b) NL2 (c) SI1 (d) SI2 (e) AR1 (f) AR2

Fig. 8. Vehicle excited by profile NL1: (a) Bridge-friendly damping coefficient to minimise DAF (b) Bridge response (── passive damping - - - bridge-friendly damping)

Fig. 9. Vehicle excited by profile SI1: (a) Bridge-friendly damping coefficient to minimise DAF (b) Bridge response (── passive damping - - - bridge-friendly damping)

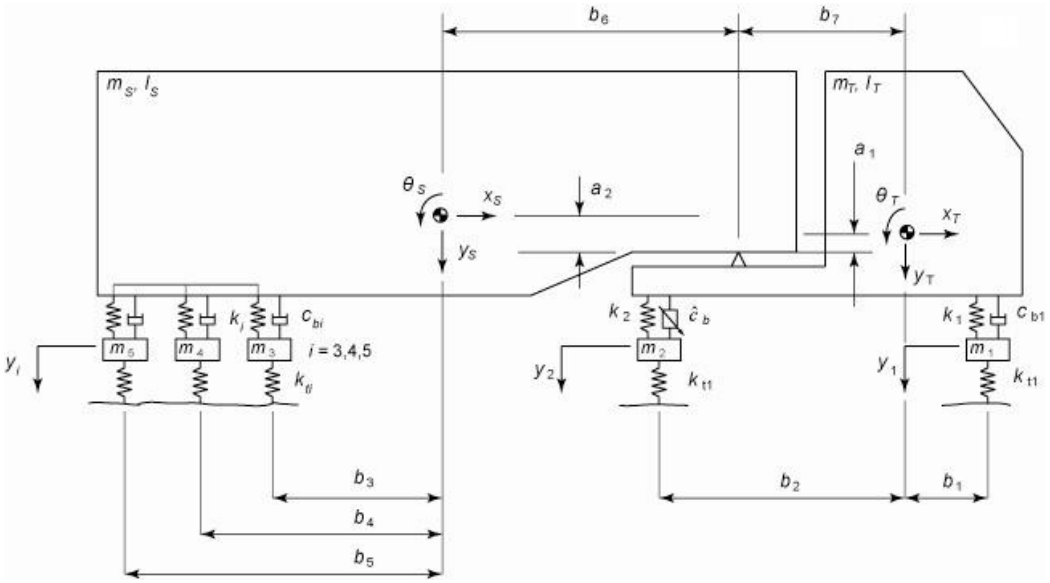
b6
b7
mS, IS
mT, IT
a1
θS
xS
a2
θT
xT
yS
yT
ki
cbi
i = 3,4,5
m5
m4
m3
kti
yi
k2
ĉb
m2
kt1
y2
k1
cb1
m1
kt1
y1
b3
b4
b5
b2
b1

Fig. 1.

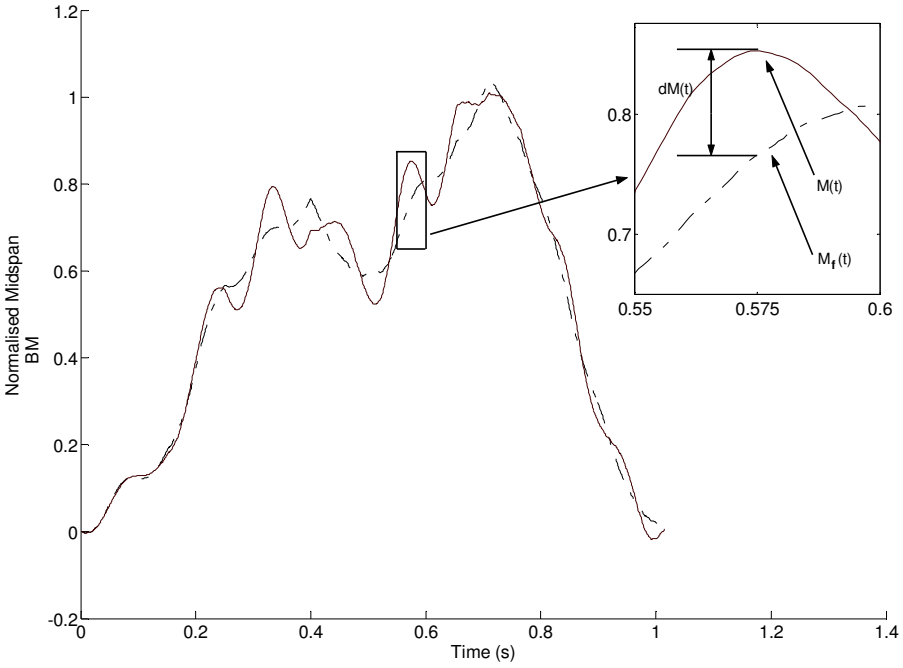

Fig. 2.

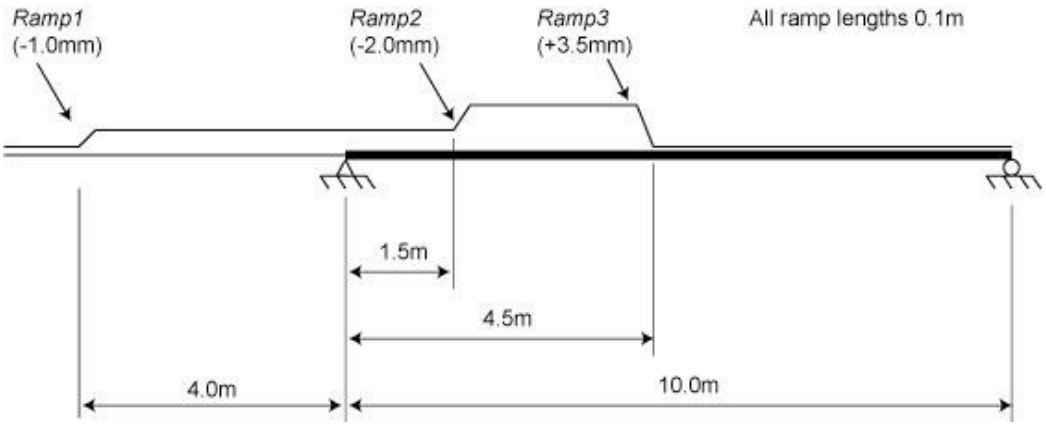
Ramp1
(-1.0mm)
Ramp2
(-2.0mm)
Ramp3
(+3.5mm)
All ramp lengths 0.1m
1.5m
4.5m
4.0m
10.0m

Fig. 3.

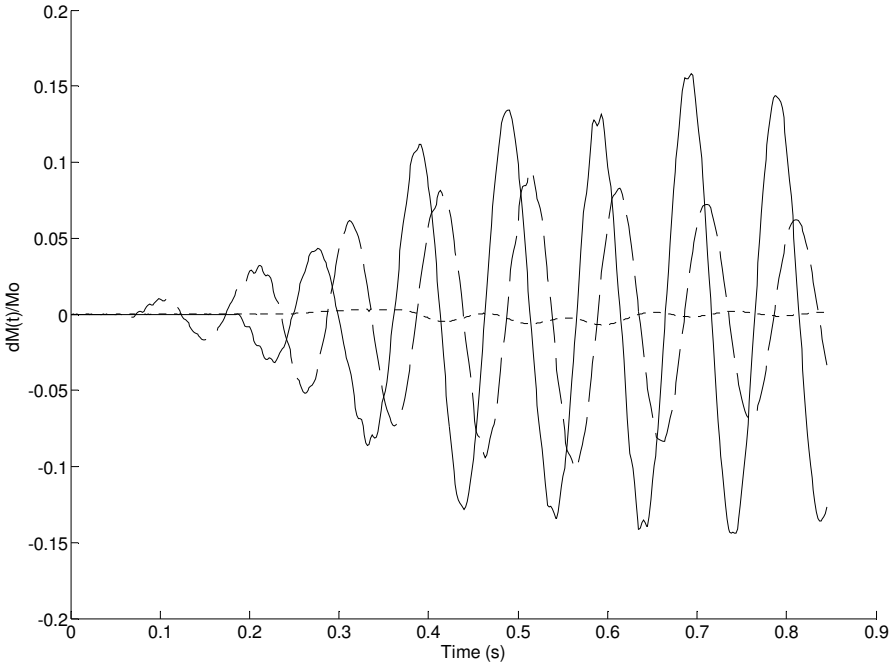
0.2
0.15
0.1
0.05
0
-0.05
-0.1
-0.15
-0.2
dM(t)/Mo
0
0.1
0.2
0.3
0.4
0.5
0.6
0.7
0.8
0.9
Time (s)

Fig. 4.

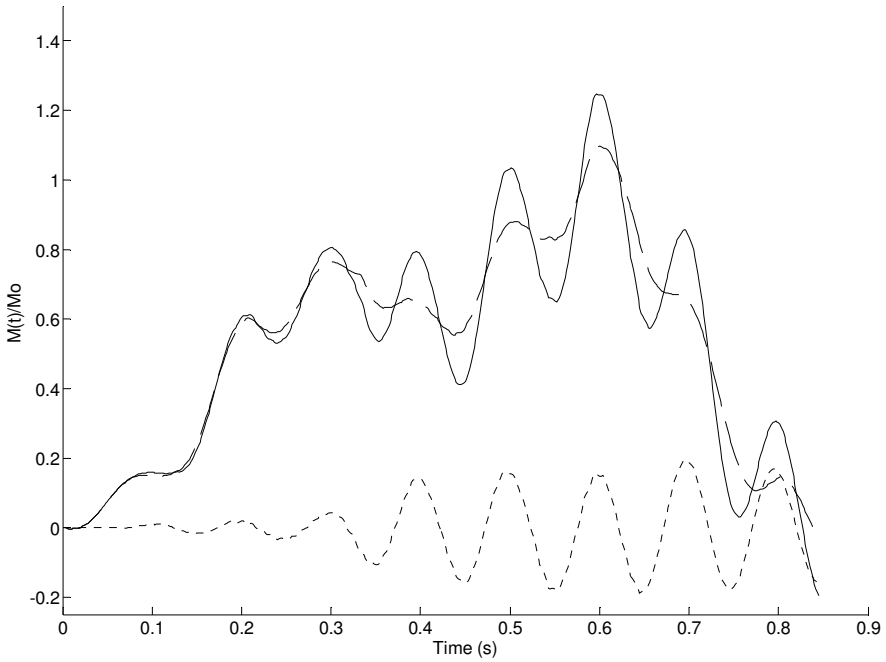

Fig. 5.

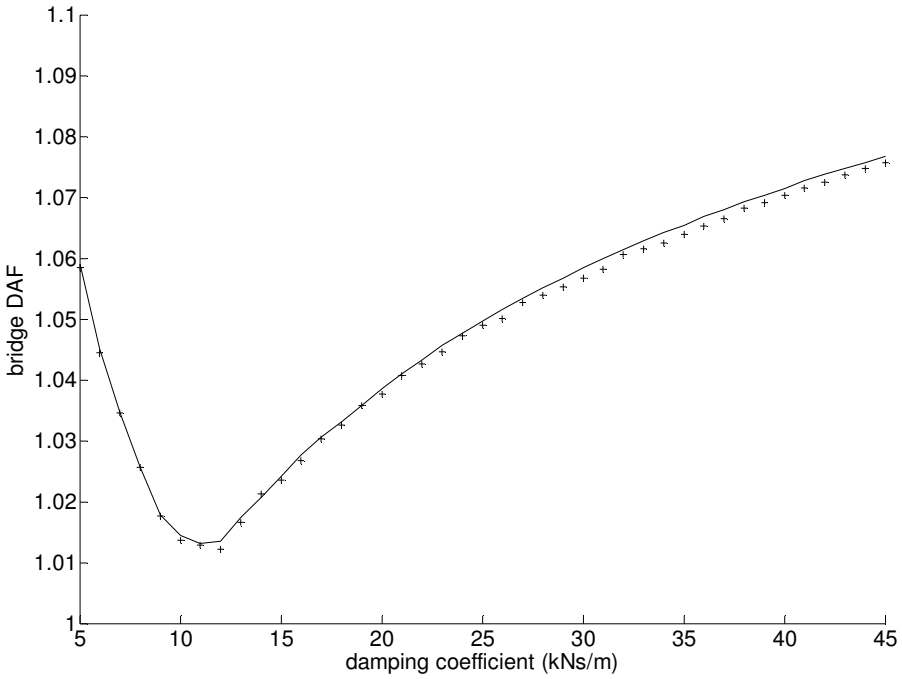
1.1
1.09
1.08
1.07
1.06
1.05
1.04
1.03
1.02
1.01
1
bridge DAF
5
10
15
20
25
30
35
40
45
damping coefficient (kNs/m)

Fig. 6.

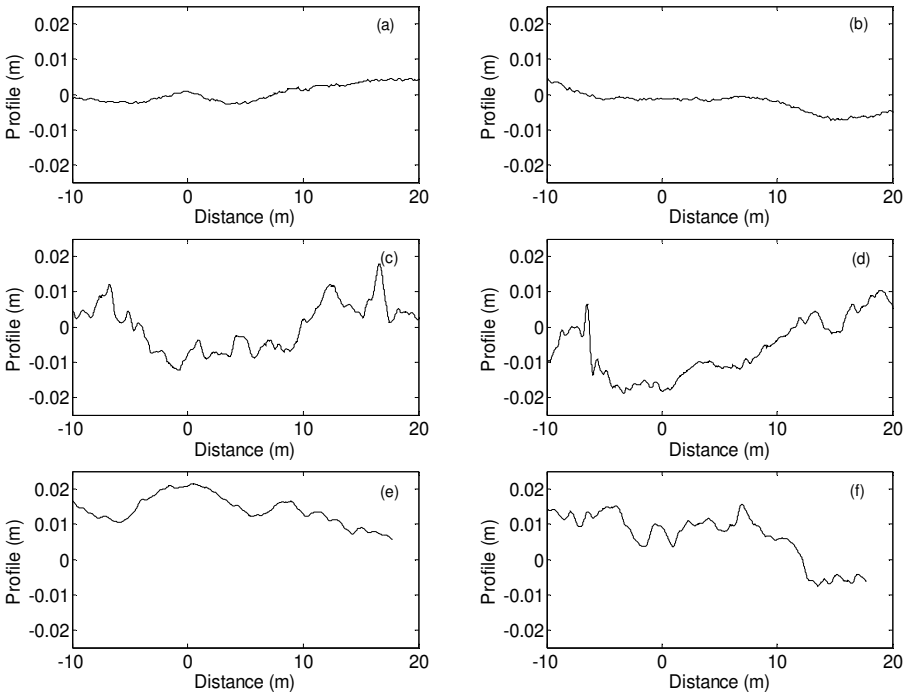

Fig. 7.

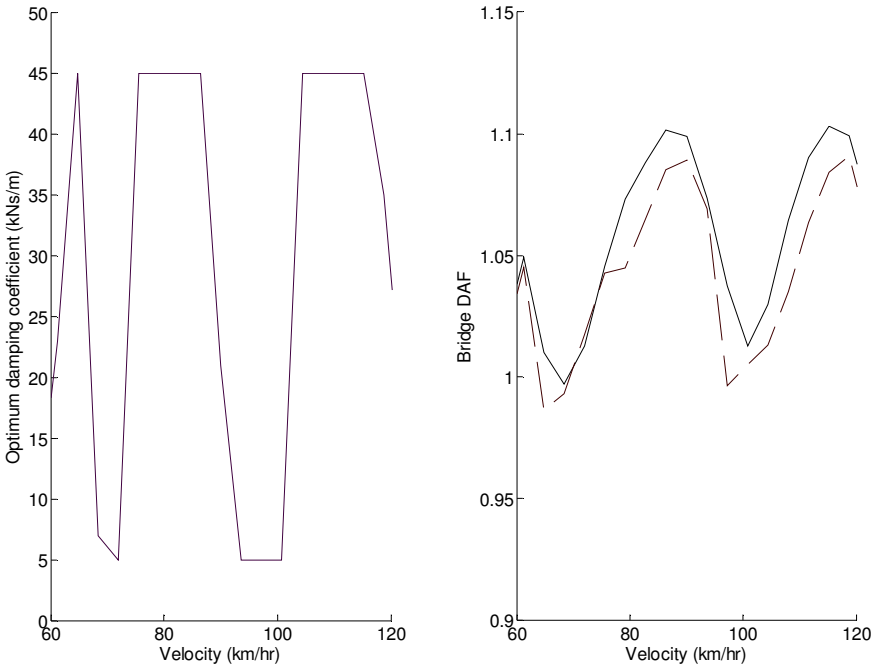
Optimum damping coefficient (kNs/m)
Velocity (km/hr)
Bridge DAF
Velocity (km/hr)

Fig. 8.

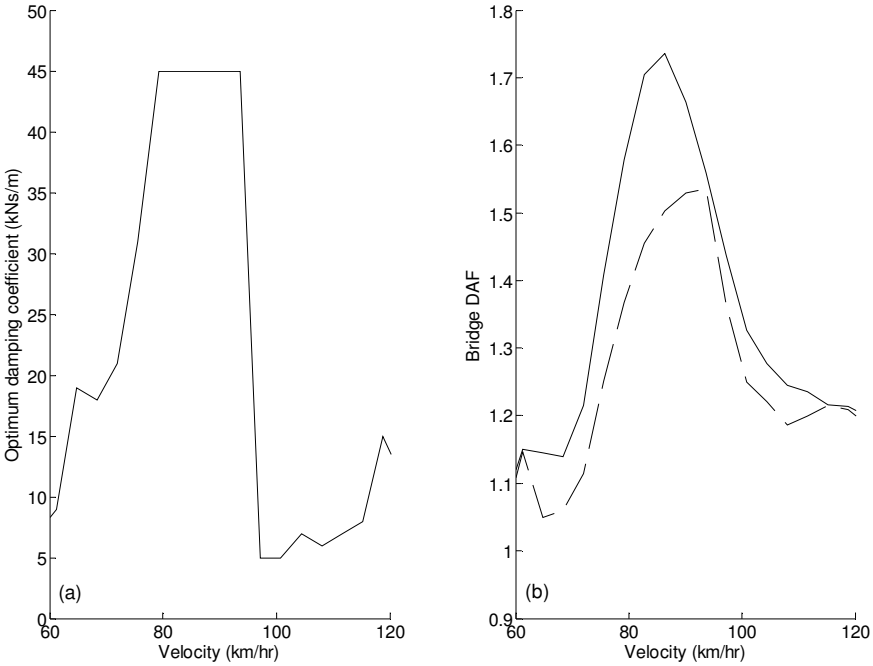
Optimum damping coefficient (kNs/m)
Velocity (km/hr)
(a)
Bridge DAF
Velocity (km/hr)
(b)

Fig. 9.

Dimensional Data *(m)*									
a_1	-0.13	a_2	1.10	b_1	0.50	b_2	2.50	b_3	1.30
b_4	2.40	b_5	3.50	b_6	4.15	b_7	2.15		

Mass and Inertia Parameters			
Mass Parameters (kg)	*Tractor sprung mass*	m_T	4500
	Semi-trailer sprung mass	m_S	31450
	Tractor front axle mass	m_1	700
	Tractor rear axle mass	m_2	1100
	Semi-trailer tridem axle mass (individual)	m_3, m_4, m_5	750
Inertia Parameters (kg m^2)	*Tractor pitch moment of inertia*	I_T	4604
	Semi-trailer pitch moment of inertia	I_S	16302

Suspension Parameters			
Spring Stiffnesses (kN/m)	*Tractor, front*	k_1	*400*
	Tractor, rear	k_2	*1000*
	Semi-trailer, tridem (individual axle)	k_3, k_4, k_5	*750*
Damping Coeffs (kNs/m)	*Tractor, front*	c_{b1}	*10*
	Tractor, rear	$\hat{c}_b$	*Variable*
	Semi-trailer, tridem (individual axle)	c_{b3}, c_{b4}, c_{b5}	*10*
Tyre Stiffnesses (kN/m)	*Tractor, front*	k_{t1}	*1750*
	Tractor, rear	k_{t2}	*3500*
	Semi-trailer, tridem (individual axle)	k_{t3}, k_{t4}, k_{t5}	*3500*

Table 1. Parameters for truck model

Road Profile	**NL1**	**NL2**	**SI1**	**SI2**	**AR1**	**AR2**
DAF - Passive Damping	1.103	1.115	1.736	1.247	1.082	1.811
DAF - Bridge-Friendly Damping	1.091	1.096	1.535	1.207	1.066	1.481
Reduction of Overall DAF	0.01%	0.02%	11.6%	0.03%	0.01%	18.2%
Reduction of Dynamic Increment	11.7%	16.5%	27.3%	16.2%	19.5%	40.7%

Table 2. Achievable reductions for each profile